Electronic structure of metal-free phthalocyanine: A valence effective Hamiltonian theoretical study

E. Ortí[a] and J. L. Brédas[b),c)]

Laboratoire de Chimie Théorique Appliquée, Centre de Recherches sur les Matériaux Avancés, Facultés Universitaires Notre-Dame de la Paix, Rue de Bruxelles, 61 B-5000 Namur, Belgium

(Received 24 December 1987; accepted 4 April 1988)

We present a valence effective Hamiltonian (VEH) nonempirical investigation of the electronic properties of metal-free phthalocyanine. The valence one-electron energy levels are related to those of the phthalocyanine components: benzene, pyrrole, and isoindole. From the electronic structure standpoint, phthalocyanine has to be viewed as formed by joining four benzene moieties to the central carbon–nitrogen ring rather than by combining four isoindole units through nitrogen bridges. Comparison of the VEH density-of-valence-states curves with the experimental ultraviolet photoelectron spectroscopy (UPS) data is quantitatively excellent and allows for a complete interpretation of the experimental spectra.

I. INTRODUCTION

Phthalocyanines have been the object of thousands of papers.[1] They correspond to macrocyclic planar aromatic compounds (see Fig. 1) which exhibit a number of unique properties making them of interest in different fields.[2] Their intense color and high thermal and chemical stability have for decades determined their use as dyes, e.g., in the textile or paint industries. Over 70 different phthalocyanine complexes MPc can be obtained by substituting the central 2 hydrogen atoms by metal or metalloid atoms. This chemical versatility provides a rich redox chemistry and makes these compounds very useful in heterogeneous catalysis, batteries, and electrochromic devices. The delocalizable π-electron system can serve as a source of charge carriers and is the origin of photoelectric properties which have been extensively studied because of their potential applications, e.g., in electrophotographic systems, photovoltaic cells, photoelectrochemical devices, or nonlinear optical devices.

Interest in phthalocyanine-based compounds has recently been renewed due to the discovery that they can form "molecular metals." Crystals of pure phthalocyanines exhibit conductivities (σ) in the insulating or semiconducting range ($\sigma < 10^{-10}$ S/cm).[3] As early as 1975, it was, however, shown that the cocrystallization of macrocycles such as diphenylglyoxamate with oxidant agents like iodine yields highly conducting materials.[4] The same redox chemistry was later applied to phthalocyanines to produce iodine oxidized crystals.[5] The electrical conductivities of these crystals are on the order of 10–1000 S/cm at room temperature and present a metallic character down to very low temperatures.

In a way similar to that in tetracyanoplatinate salts,[6] partially oxidized phthalocyanines crystallize in columns along which macrocycles are stacked face-to-face.[5] Such a crystal packing leads to weak interactions between neighboring stacks and produces a highly anisotropic conductivity. Unlike the situation in tetracyanoplatinate salts where electrons mostly move through the chain of Pt atoms, the presence of metal atoms is not a requirement to achieve high conductivities in phthalocyanines, since the interaction between π-molecular orbitals on adjacent macrocycles facing one another can provide the electronic pathway. The stacking distance being around 3.2–3.4 Å, the interactions between the molecules are mostly of van der Waals type. Therefore, the electronic and structural characteristics of the molecule remain almost unaffected in the crystalline state. Thus, the determination of the electronic structure of the isolated metal-free phthalocyanine molecule constitutes a crucial step towards the understanding of the electronic properties of phthalocyanine-based compounds.

Since the first calculation of Pullman and Berthier in 1953,[7] the electronic structure of the phthalocyanine molecule has been studied in the framework of Hückel,[8] extended Hückel,[9] Pariser–Parr–Pople (PPP),[10] and complete ne-

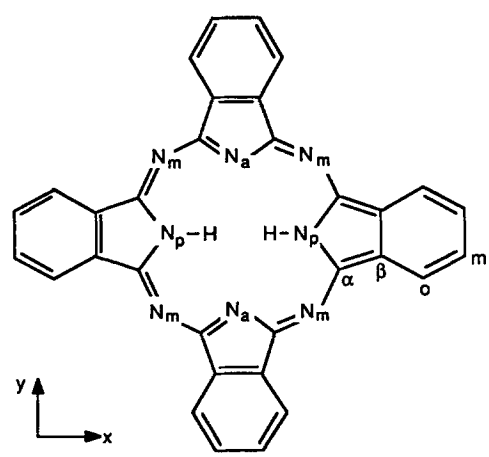

FIG. 1. Molecular structure of metal-free phthalocyanine. N_p denotes a pyrrole nitrogen and N_a and N_m denote pyrrole aza and meso-bridging aza nitrogens, respectively. The carbon atoms are denoted following their position with respect to pyrrole nitrogen atoms (C_α and C_β) and to the pyrrole moiety (C_o and C_m).

[a] Permanent address: Departamento de Química Física, Facultad de Química, Universidad de Valencia, Dr. Moliner, 50, 46100-Burjassot (Valencia), Spain.

[b] Maître de Recherches of the Belgian National Fund for Scientific Research (FNRS).

[c] New permanent address: Service de Chimie des Matériaux Nouveaux, Université de l'Etat à Mons, avenue Maistriau 21, B-7000 Mons, Belgium.

 0021-9606/88/141009-08$02.10

glect of differential overlap (CNDO)[11] approaches. However, all those studies mainly focused on the highest occupied energy levels in order to interpret the optical properties observed from gas-phase absorption spectra and did not pay much attention to the lower-lying energy levels. Several papers have been published on the solid-state photoemission [ultraviolet photoelectron spectroscopy (UPS) or x-ray photoelectron spectroscopy (XPS)] spectra of phthalocyanine films.[12] Only one detailed study has recently been reported by Berkowitz on the gas-phase UPS spectra of metal-free and metallophthalocyanine molecules.[13] In that work, the photoemission bands were assigned by comparison with solid state spectra and previously reported calculations on porphyrins. In his conclusion, Berkowitz called for reliable theoretical calculations on phthalocyanine in order to assess the validity of his assignments. The only theoretical attempt to interpret the UPS spectra of Berkowitz has actually been performed on a related simpler macrocycle, metal-free tetraazaporphyrin, using the one-electron Hartree–Fock–Slater model.[14]

The purpose of this paper is to perform a comprehensive theoretical analysis of the whole valence electronic structure of metal-free phthalocyanine (H_2Pc). Our goal is to give a detailed interpretation of the available gas-phase UPS spectrum of H_2Pc and also to provide a theoretical framework allowing the comparison with solid state data (as well as possible future gas-phase XPS measurements on H_2Pc). The large size and complexity of phthalocyanine, $C_{32}H_{18}N_8$, makes it rather difficult to apply standard *ab initio* methods to calculate its electronic structure. To the best of our knowledge, only one nonempirical study has been reported so far on a phthalocyanine compound, namely nickel phthalocyanine, using the discrete variational X-α technique.[15] In this work, we make use of the nonempirical VEH pseudopotential method. A brief outline of our methodology is presented in Sec. II. Results are reported and discussed in Sec. III and conclusions are given in Sec. IV.

II. METHODOLOGY

All the calculations reported in this paper have been performed in the framework of the VEH quantum-chemical technique. The VEH method has been originally developed for molecules by Nicolas and Durand[16] and extended for polymers by André *et al.*[17] The method is based on the use of an effective Fock Hamiltonian F_{eff} which combines a kinetic term and a summation over atomic potentials. All the parameters entering the atomic potentials are optimized on model molecules in order to minimize the difference between F_{eff} and the Fock Hamiltonian built from Hartree–Fock *ab initio* double-zeta calculations. In this way, the VEH method is completely nonempirical and yields one-electron energy levels of *ab initio* double-zeta quality. The VEH atomic potentials used in this work are those previously optimized for hydrogen, carbon, and nitrogen.[18,19]

From the VEH one-electron energy results [eigenvalue ϵ_i in the molecular case or band structure $\epsilon_i(k)$ in the polymer case], it is possible to simulate theoretically the photoemission (UPS and/or XPS) spectrum of a given molecule or polymer. Up to now, this simulation has mostly been performed for polymers (such as polyacetylene,[18] polyparaphenylene,[20] polybenzothiophene,[21] polystyrene,[22] or polyacrylonitrile[23]) and has afforded an excellent comparison with experimental UPS and XPS data. In the case of molecules, the simulation of a UPS spectrum simply requires that each eigenvalue ϵ_i be convoluted by a Gaussian function I_i:

$$I_i(\epsilon) = e^{-(\epsilon-\epsilon_i)^2/\gamma} \tag{1}$$

whose full width at half-maximum is adjusted by $\gamma(\gamma = \omega^2/4 \ln 2, \omega$ being the desired width). The total intensity at each point on the energy scale is the summation over all the Gaussian functions at that particular point:

$$I(\epsilon) = \sum_i I_i(\epsilon). \tag{2}$$

To simulate an XPS spectrum, an additional factor α_i is introduced in Eq. (1) to modulate the intensity of each Gaussian function. We have used the cross section model of Gelius,[24] where the intensity factor α_i is related to the Mulliken gross atomic population[25] and experimental photoemission cross sections σ_p of atomic orbitals:

$$\alpha_i = \sum_p c_{ip}\left[\sum_q S_{pq} c_{iq}\right]\sigma_p. \tag{3}$$

In Eq. (3), the summations over p and q run over all atomic orbitals; c_{ip} refers to the LCAO (linear combination of atomic orbitals) coefficient of atomic orbital p in the ith molecular orbital; and S_{pq} denotes the overlap integral between atomic orbitals p and q.

The Gaussian convolution process is performed with a full width at half-maximum of 0.7 eV, which is the value most generally used in previous VEH simulations of UPS or XPS solid-state spectra. A smaller value of 0.4 eV is also employed to account for the higher resolution of the gas-phase UPS spectra. As is often the case in the framework of *ab initio* techniques, VEH yields too wide a valence electronic structure and a contraction of the energy scale becomes necessary to obtain the best fit between theoretical one-electron energy levels and experimental UPS or XPS peak positions. The contraction factor generally varies with the system under study. However, a value of 1.3 has been used in almost all the comparisons which have been previously made between VEH calculated and experimental photoemission spectra.[18,20–23] For the sake of consistency, we have considered the same 1.3 factor in this work.

The geometrical structure of metal-free phthalocyanine has been investigated only in the solid state. As early as 1935,[26] Robertson performed an x-ray diffraction study of the lattice parameters of the β-polymorphic form and a year later reported a detailed structure of the carbon–nitrogen skeleton of the molecule.[27] More recently, Hoskins *et al.*[28] carried out a neutron diffraction study on the same β polymorphic form. Both works agree in attributing a planar C_{2h} geometry to the H_2Pc molecule. However, the location of the inner two hydrogen atoms is not well defined. From the x-ray data, a hydrogen-bridged model was proposed where each hydrogen is shared by two neighboring nitrogen atoms.[27,29] On the contrary, from the neutron diffraction data, a hydrogen-bonded model was suggested where the central two hydrogens are localized on opposite nitrogen

atoms.[28] Many papers have dealt with this controversy and both geometric structures have been used in theoretical studies.[8–11,14] In our work, we have assumed the hydrogen-bonded structure shown in Fig. 1. The hydrogen-bonded structure is indeed further supported by XPS measurements of the nitrogen 1*s* level splitting which unambiguously demonstrate that, among the pyrrole-like rings, there exist two types of nitrogens: two pyrrole (N_p) nitrogens and two aza (N_a) nitrogens (see Fig. 1).[30] To define the molecular geometry, we have used the neutron diffraction interatomic distances and angles.[28] The calculations have been performed both on the reported C_{2h} geometry and on an averaged D_{2h} structure. The D_{2h} atomic coordinates have been obtained by taking the arithmetic means of the experimental values for equivalent bonds on opposite isoindole moieties in order to impose symmetry planes passing through the central nitrogens. Since both geometries lead to identical results, only the results of the calculations based on D_{2h} symmetry are presented in Sec. III.

In Sec. III, we also include VEH calculations on benzene, pyrrole, and isoindole. These smaller molecules are components of the phthalocyanine macrocycle and have been studied for the following reasons: (i) In order to facilitate the analysis of the electronic structure of the phthalocyanine molecule since it must be borne in mind that there are 93 occupied molecular orbitals in the valence electronic structure of H_2Pc; and (ii) in order to assess further the quality of VEH calculations, since detailed theoretical and experimental data are available for these smaller systems.

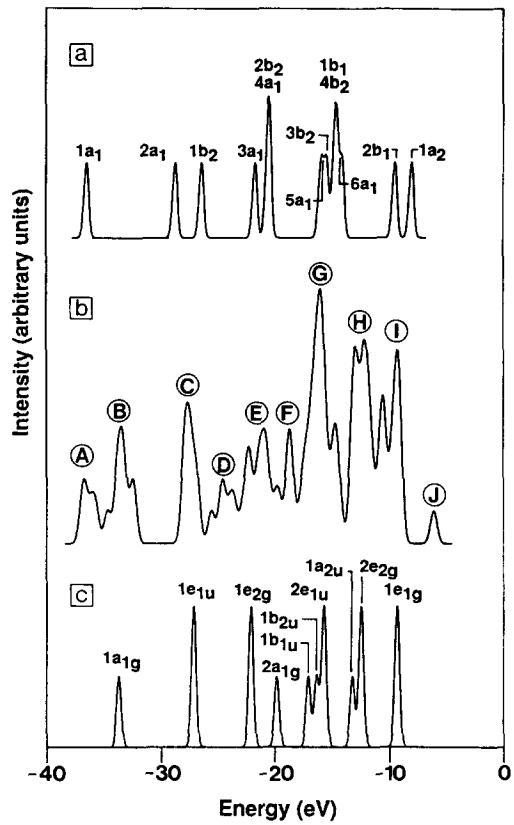

FIG. 2. VEH theoretical simulation of the UPS spectrum for (a) pyrrole, (b) metal-free phthalocyanine, and (c) benzene. The symmetries of the molecular orbitals giving rise to the different peaks are indicated for benzene and pyrrole. The molecular orbitals are numbered starting with the lowest-lying valence orbital. Convolutions of the electronic levels are performed by Gaussians with full width at half-maximum of 0.7 eV.

III. RESULTS AND DISCUSSION

A. Theoretical UPS spectrum

The VEH electronic density-of-valence-states (DOVS) spectra obtained for D_{2h} metal-free phthalocyanine, benzene, and pyrrole are presented in Fig. 2 and Table I. The spectra in Fig. 2 constitute a theoretical simulation of the photoemission UPS spectra. They are obtained following the methodology discussed above using a full width at half-maximum of 0.7 eV for the Gaussian functions. The peak structures appearing for H_2Pc in Fig. 2(b) are identified by labels from A to J. These labels are used in Table I (where the energies of the different peaks are listed for H_2Pc) and in the following discussion. In the case of benzene and pyrrole, gas-phase geometries have been used in the VEH calculations.[31,32] At first glance, nearly all the main structures of the phthalocyanine spectrum can be correlated with peaks appearing either in benzene or pyrrole.

We now discuss in detail the origin of each H_2Pc peak in Fig. 2(b) and the relationships with benzene or pyrrole molecular orbitals. Structure A in Fig. 2(b) comes from the 2*s* atomic orbitals of the N_p, N_a, and C_α atoms. This orbital composition is similar to that of the $1a_1$ molecular orbital of pyrrole, the splitting of the peak in H_2Pc being due to the different N_p and N_a molecular environments. The three-peak structure of B results from contributions of 2*s* orbitals of benzene carbon atoms and all nitrogen atoms. More precisely, the main peak at -33.47 eV corresponds to a strongly bonding interaction between the benzene carbon atoms ($1a_{1g}$ molecular orbital of benzene) and the shoulders originate in the 2*s* orbitals of N_m (high binding energy side) and N_p–N_a (low binding energy side) atoms, respectively.

TABLE I. VEH energies (in eV) corresponding to the peaks in the valence electronic density of states spectrum displayed in Fig. 2(b) for metal-free phthalocyanine. See Fig. 2(b) for labels.

Structure	Energy
A	−36.72
	−35.98
B	−34.64
	−33.47
	−32.49
C	−27.67
D	−25.55
	−24.58
	−23.77
E	−22.24
	−20.92
	−19.78
F	−18.67
G	−15.92
	−14.70
I	−10.60
	−9.22
J	−6.15

Broad peak C involves eight different molecular orbitals where the main contributions are from C_0 or C_β and $C_m 2s$ orbitals, much as in the degenerate $1e_{1u}$ molecular orbitals of benzene. Peak D has no correspondence to benzene or pyrrole and mainly comes from $C_\alpha 2s$ orbitals. All three peaks constituting structure E are associated with benzene atoms: (i) the first peak at -22.24 eV has the same atomic composition as the degenerate $1e_{2g}2s$ orbitals of benzene; (ii) the peak at -19.78 eV corresponds to the C_0–H bonds as in the benzene $2a_{1g}$ orbital; (iii) both $1e_{2g}$ and $2a_{1g}$ orbitals are present in the highest peak at -20.92 eV where some contribution from nitrogen atoms is also detected. The molecular orbitals that give rise to peak F are mainly due to $2p\,\sigma$ molecular orbitals from the nitrogen and carbon atoms forming the central ring of phthalocyanine.

We now analyze the atomic composition of the outer part of the valence electronic structure which can be correlated with the experimental gas-phase UPS spectrum. The most intense peak in the theoretical spectrum (peak G) is located at -15.92 eV and has a very broad structure resulting from the convolution of 18 molecular orbitals under it. On the high binding energy side, a group of four molecular orbitals composed of $2s$ (carbon) and $1s$ (hydrogen) orbitals of benzene atoms is found. These orbitals are of the same nature as the $1b_{1u}$ molecular orbital of benzene and cause the appearance of two shoulders (which can be easily seen in Fig. 5 where a smaller convolution factor has been used). The other molecular orbitals are formed by $1s$, $2p_x$, and $2p_y$ atomic orbitals building the ring and C–H σ structure of the benzene moieties. The composition of these molecular orbitals is the same as that of the $1b_{2u}$ and $2e_{1u}$ benzene molecular orbitals which are energetically located around the -15.92 eV H_2Pc peak (-16.33 and -15.70 eV, respectively). Three π orbitals coming from all nitrogen and C_α atoms also contribute to peak G. The shoulder to the right of structure G can be attributed to the totally bonding $1b_1\pi$ orbital of pyrrole although significant contributions from the σ structure of benzene rings are also detected.

Structure H involves two peaks resulting from a mixing of benzene moieties and nitrogen atoms. The peak at higher binding energy originates in the totally bonding π interaction of benzene carbon atoms with some contribution from $N_m 2p_z$ orbitals and can be clearly correlated with the $1a_{2u}$ π molecular orbital of benzene. The other peak at higher energy is mainly due to N_a lone pairs but important contributions from C–C and C–H benzene bonds ($2e_{2g}$ molecular orbitals) are also observed. The origin of the peaks involved in structure I is clearly defined. The first peak at -10.60 eV corresponds to the σ lone pairs of N_m atoms. The second peak at -9.22 eV is of π nature and results from the highest occupied (degenerate) $1e_{1g}$ orbitals of benzene with some contributions from N_p and N_a atoms.

Finally, small peak J has no correspondence at all in the pyrrole or benzene spectra. It comes only from the $4a_u$ highest occupied molecular orbital (HOMO) of the phthalocyanine molecule. This orbital is located at -6.15 eV and lies 3 eV above the $7b_{1u}$ next-to-last occupied molecular orbital. No nitrogen atom contributes to the electronic distribution of the $4a_u$ orbital which is therefore confined within the isoindole moieties as sketched below:

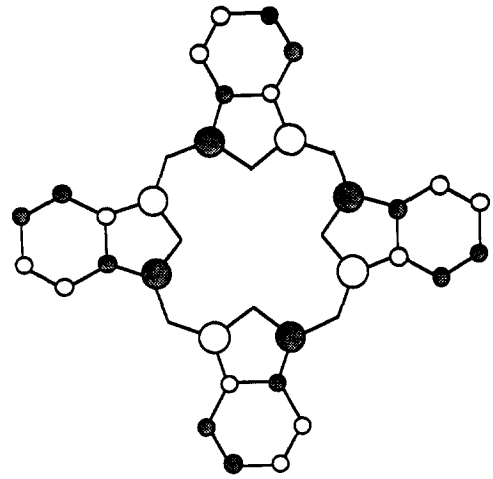

From the preceding analysis, it is clear that all the orbitals of the benzene molecule are present in the electronic structure of metal-free phthalocyanine. Thus, the characteristics of the electronic structure of the benzene moieties are conserved in the phthalocyanine macrocycle and a simple correlation between the one-electron energy levels of both molecules can be established. On the contrary, almost no molecular orbitals pertaining to pyrrole can be identified in the H_2Pc electronic structure and it is the central macrocycle backbone which mostly accounts for the electronic contributions of N_p, N_a, and C_α atoms. As a consequence, we have to conclude that the definition of phthalocyanine in terms of four isoindole units linked by aza nitrogen atoms is not valid. From an electronic structure standpoint, the phthalocyanine molecule must rather be visualized as the result of joining four benzene rings to the central carbon–nitrogen macrocycle (with the exception of the HOMO).

These conclusions are further supported by a comparison of the geometries found in the isoindole moiety of phthalocyanine and isoindole itself. These geometries are illustrated in Fig. 3 together with that of pyrrole. (In the case of phthalocyanine, the geometry results from averaging over the four isoindole units.) The geometry of CoPc has also been included because it is one of the phthalocyanine struc-

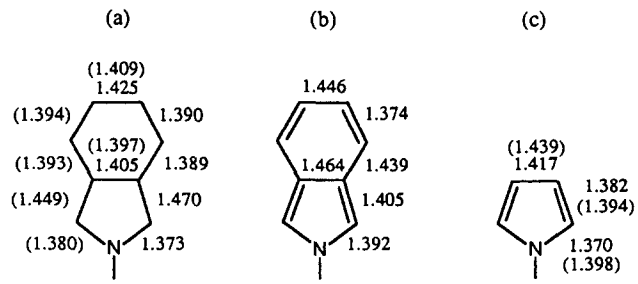

FIG. 3. Comparison of bond lengths (in Å) in isoindole and related compounds: (a) experimental (averaged) bond lengths for the isoindole units in H_2Pc (Ref. 27) [the values for CoPc (Ref. 32) are given in parentheses]; (b) bond lengths in the isoindole molecule as obtained from a semiempirical Hartree–Fock MNDO geometry optimization; (c) experimental (microwave) bond lengths in pyrrole (Ref. 31) [MNDO-optimized values in parentheses (Ref. 19)].

tures determined most accurately.[33] The modified neglect of diatomic overlap (MNDO) optimized geometry is shown for isoindole since no experimental data are available for that molecule. There are marked differences between the geometry of isoindole units within phthalocyanine and that of the isoindole molecule. In the latter case, the bond length values define a strongly alternated structure with double bonds joining C_α–C_β and C_0–C_m atoms. Thus, the structure of pyrrole is mainly retained in the isoindole molecule and isoindole can be considered as resulting from the fusion of pyrrole ring with 1,3-butadiene. The situation is opposite in phthalocyanine since the isoindole units of H_2Pc possess almost equal bond lengths (around 1.4 Å) for all benzene carbon–carbon bonds and the C_α–C_β bonds have mostly single-bond character. The geometry of pyrrole is not preserved here and the isoindole units of H_2Pc correspond to nearly atomic benzene rings fused on top of a methineimine-like chain.

It is also important to note the very small differences between the isoindole structures containing N_p and N_a atoms in H_2Pc. The maximum deviation from the averaged values summarized in Fig. 3(a) is only on the order of ± 0.02 Å for H_2Pc and about ± 0.01 Å for CoPc. This observation is consistent with the very fast N–H tautomeric process due to the exchange of the central hydrogen atoms between the N_p and N_a nitrogens.[34] As a consequence, metal-free phthalocyanine presents a fully delocalized structure almost identical to the D_{4h} geometry of metallophthalocyanines.

B. Theoretical XPS spectrum

The theoretical XPS spectrum of metal-free phthalocyanine (as obtained from convolution by Gaussians with full width at half-maximum of 0.7 eV) is displayed in Fig. 4. The spectrum shows the same overall features as the UPS simulation (Fig. 2) but the relative intensities of the peaks are dramatically changed. As a consequence of the much larger x-ray photoemission cross sections of carbon and nitrogen 2*s* atomic orbitals relative to 2*p* atomic orbitals,[24] the most intense peaks in the XPS spectrum are to be found in the deepest part of the valence region. The positions and assignments of the peaks are the same as for the UPS spectrum and only two peaks experience some shift. The central peak of structure E is now located at -21.15 eV instead of -20.92 eV in the UPS theoretical spectrum. This slight shift is due to the fact that the UPS peak comes from both carbon 2*s* ($1e_{2g}$) and 2*p* ($2a_{1g}$) benzene orbitals whereas the XPS peak is mainly determined from the carbon 2*s* orbitals which lie at lower energies. A larger change is obtained for the most intense peak in the UPS spectrum which shifts down to -16.91 eV from -15.92 eV. This evolution originates in the presence of strong contributions from carbon 2*s* ($1b_{1u}$) orbitals of the benzene moieties on the high-binding energy side of the peak. Finally, it must be noted that the intensity of the highest energy peak corresponding to the $4a_u$ HOMO level is very small, in agreement with the π nature of that orbital. This provides an explanation for the disappearance of this peak in metal-free phthalocyanine films when passing from UPS to XPS.[12]

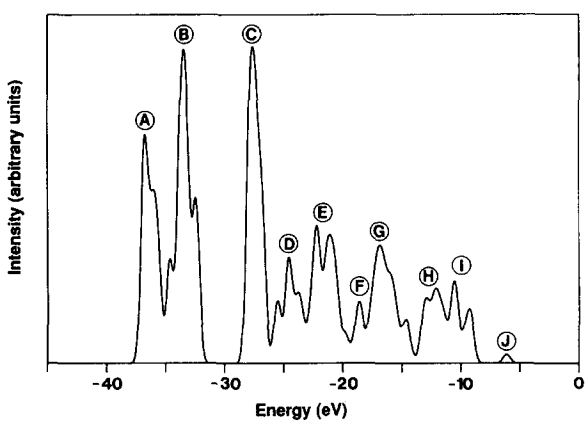

FIG. 4. VEH theoretical simulation of the XPS spectrum of metal-free phthalocyanine. A value of 0.7 eV is used for the full width at half-maximum of the convoluting Gaussian functions. Labels are the same as in Fig. 2(b).

C. Correlation with experimental data: Benzene, pyrrole, and isoindole

One of the main sources of experimental data for the valence electronic structure of phthalocyanine is the gas-phase UPS spectrum reported by Berkowitz.[13] This spectrum provides information on a narrow range of energies, down to 14 eV in binding energy. Consequently, the correlation with our theoretical results is limited. It is therefore of interest to carry out a study of the results that VEH yields for smaller relevant systems such as benzene and pyrrole, for which the whole electronic structure has been experimentally investigated. In doing so, we aim at testing the reliability of VEH calculations and its usefulness in interpreting the phthalocyanine UPS spectrum of Berkowitz.

The VEH valence one-electron energy levels of benzene and pyrrole are listed in Table II together with their symmetries (within D_{6h} and C_{2v} groups, respectively). The VEH valence electronic structure is contracted by a factor of 1.3, as discussed above, without applying any shift of the origin. In Table II, we also include the experimental (vertical) ionization potentials obtained from gas-phase photoemission measurements.[35] Although many a theoretical calculation has been reported in the literature for benzene and pyrrole, we only list in Table II the energy levels calculated by von Niessen *et al.*[36,37] These are of special interest since electron correlation and reorganization effects are included by means of a many-body Green's function technique.

As can be seen from Table II, the agreement between the VEH energy level distribution and the experimental data is extremely good for benzene. The VEH theoretical symmetry ordering correlates perfectly with the experimental assignments and the ordering reported by von Niessen *et al.*[36] If we exclude the lowest-lying level (which is generally calculated to be too low in energy when using the VEH technique for hydrocarbons, as reported previously[18]), the standard deviation between the VEH and experimental data is as small as 0.15 eV. We stress that an excellent agreement is found in particular for the upper four levels which are theoretically

TABLE II. VEH theoretical ($-\epsilon_i$) and experimental one-electron energy levels for benzene and pyrrole. Energies are in eV.

	Symmetry[a]	VEH[b]	Expt.[c]	*Ab initio*[d]
Benzene	$1a_{1g}$	28.09	25.9	
	$1e_{1u}$	23.04	22.7	
	$1e_{2g}$	19.14	19.0	19.97
	$2a_{1g}$	17.39	17.0	17.28
	$1b_{1u}$	15.28	15.7	15.82
	$1b_{2u}$	14.72	14.9	14.64
	$2e_{1u}$	14.23	14.2	14.30
	$1a_{2u}(\pi)$	12.33	12.3	12.02
	$2e_{2g}$	11.74	11.8	11.94
	$1e_{1g}(\pi)$	9.35	9.4	8.87
Pyrrole	$1a_1$	29.92	29.5	
	$2a_1$	23.98	23.8	
	$1b_2$	22.18	22.3	
	$3a_1$	18.56	18.8	19.64
	$2b_2$	17.71	18.1	18.96
	$4a_1$	17.59	17.5	18.17
	$5a_1$	14.14	14.8	14.86
	$3b_2$	13.77	$14.3(1b_1)$	14.37
	$1b_1(\pi)$	13.25	$13.7(3b_2)$	13.70
	$4b_2$	13.09	13.0	13.39
	$6a_1$	12.72	12.6	12.98
	$2b_1(\pi)$	9.21	9.2	8.92
	$1a_2(\pi)$	8.10	8.2	8.17

[a] The molecular orbitals are numbered starting with the lowest-lying valence molecular orbital.
[b] The total VEH valence electronic structure is contracted by a factor of 1.3 (see the text).
[c] Gas-phase UPS and XPS data from Ref. 34.
[d] Hartree–Fock double-zeta *ab initio* and many-body Green's function approach (Refs. 35 and 36).

positioned within less than 0.1 eV from the experimental ionization potentials. This feature is especially significant in relation to the H_2Pc case since: (i) these levels define the energy range covered in the UPS spectrum of Berkowitz; and (ii)the benzene moieties mainly determine the electronic structure of H_2Pc, as we pointed out before.

The VEH results for pyrrole are also in very good agreement with experimental data. This is, however, an expected feature since pyrrole served as a model molecule to parametrize the VEH nitrogen atomic potential.[19] The standard deviation between the VEH and experimental energies is about 0.2 eV. The largest differences in level positions and symmetry assignments are found in the range between 13 to 15 eV in binding energy. It must be stressed that the peak assignments are especially difficult in this region since the experimental spectrum broadens into one continuous band.[38] The VEH symmetry ordering is in complete agreement with that obtained from the accurate calculations of von Niessen *et al.*[37]

We have also calculated the VEH electronic structure of isoindole on the basis of the MNDO optimized geometry. Due to its high reactivity, no experimental data are available for isoindole and only the energies of the three highest π levels are reported for the *N*-methyl-isoindole derivative.[39] The VEH one-electron energies for those levels, after applying a contraction factor of 1.3, are 6.97 ($2a_2$), 8.62 ($3b_1$), and 9.35 eV ($1a_2$). These values correlate very well with the experimental values (7.12, 8.35, and 9.42 eV) and the larger difference found for the $3b_1$ level is due to the effect of the extra methyl group. Indeed, a VEH calculation on *N*-methyl-isoindole locates that orbital at 8.47 eV, without affecting the other energy levels.

The results discussed in this section illustrate the adequacy of the VEH technique to calculate the electronic structure of aromatic systems and validate the VEH results obtained for metal-free phthalocyanine.

D. Correlation with experimental data: Metal-free phthalocyanine

In Fig. 5, we compare the upper part of the VEH DOVS spectrum for metal-free phthalocyanine with the gas-phase UPS spectrum reported by Berkowitz.[13] The theoretical spectrum is contracted by a factor of 1.3 along the energy scale and shifted by 0.26 eV to higher binding energies to fit the first UPS peak located at 6.41 eV. The resulting peak energies are collected in Table III together with the experimental peak assignment. The binding energies obtained from the solid-state UPS spectrum on H_2Pc films reported by Tegeler *et al.*[12(c)] are also included in Table III for comparison. The energy scale is also shifted in the latter case to match the first peak of the gas-phase spectrum.

As can be seen from Fig. 5 and Table III, the correlation between the theoretical and experimental spectra is not always obvious. While for some peaks a quantitative agreement is found, no correspondence is observed for other peaks. These discrepancies call for a detailed discussion of the interpretation of the experimental spectrum.

The first peak at 6.41 eV unambiguously corresponds to

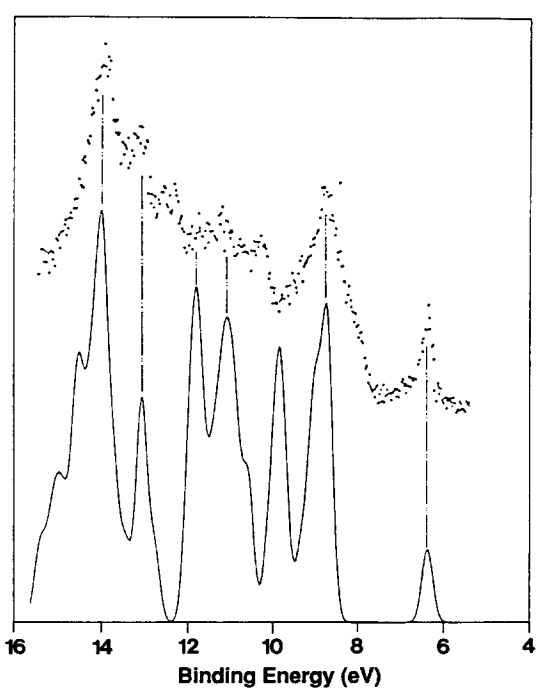

FIG. 5. Comparison of the VEH theoretical photoemission spectrum (solid line) with the gas-phase UPS spectrum (Ref. 13) of metal-free phthalocyanine. (The theoretical spectrum is contracted by a factor of 1.3 and shifted 0.26 eV to higher binding energies. Gaussians with full width at half-maximum of 0.4 eV are used in the convolution process.)

TABLE III. Comparison of VEH theoretical and experimental valence energy levels of metal-free phthalocyanine. (Energies are in eV.)

Gas phase[a]	VEH[b]	Solid state[c]
6.41 s	6.41 (J)	6.4
8.75 b	8.77 (I)	9.1
	9.83	
10.24 wp		
11.2 (?)pw	11.06 (H)	11.5
	11.74	
12.27 pw		
12.57 pw		
13.12 dp	12.99 (G)	
13.92 dp	13.92	14.1
	16.04 (F)	15.8
	17.77 (E)	18.5
	18.77	
	20.59 (D)	
	22.96 (C)	22.4
	27.42 (B)	25.4
	29.36 (A)	28.7
	29.93	

[a] Gas-phase He-I UPS data (Ref. 13). Notation is: s = sharp, b = broad peak, wp = weak plateau, pw = possible weak peak, dp = distinct peak.
[b] The VEH energy scale is contracted by a factor of 1.3 and shifted by 0.26 eV towards higher binding energies in order to match the first gas-phase peak. Only the most intense peaks are included for high binding energies (See Fig. 2 for labels.)
[c] Solid state synchrotron (photon energy = 100 eV) UPS data [Ref. 12(c)]. Values are shifted by 0.5 eV towards higher binding energies.

the ionization of the $4a_u$ highest occupied molecular orbital. In relation with this peak, Berkowitz also suggests the existence of a shoulder at higher binding energies. This shoulder was quantitatively measured for some metallophthalocyanines and is assigned to a second macrocycle orbital on the basis of *ab initio* and *X-α* calculations reported for porphyrins.[40,41] However, this assignment is not correct since metal-free porphyrin (H_2P) and H_2Pc show a markedly different electronic structure near the HOMO. In accord with previous calculations,[40,41] VEH results confirm that a second orbital lies only 0.5 eV below the HOMO level in H_2P.[42] On the contrary, H_2Pc exhibits a very large gap of ≈ 3 eV between the HOMO and the following orbital. Therefore, this shoulder, when present in phthalocyanine compounds, can only be related to metal orbitals or impurities.

After an important energy gap, a very broad band is experimentally detected, which peaks at 8.75 eV in perfect agreement with the theoretical value of 8.77 eV. As was discussed in Sec. III A, this peak comes from the benzene π orbitals. A series of possible weak peaks is suggested between 10 and 13 eV and will be discussed below. Two distinct peaks are finally reported at 13.12 and 13.92 eV which correlate perfectly with the theoretical peaks at 12.99 and 13.92 eV, respectively. At both theoretical and experimental levels, the peak at 13.92 eV is found to be the most intense in the spectrum and corresponds to the C–C and C–H σ bonds of the benzene moieties (see Sec. III A).

We now turn to a discussion of the peaks in the 10–13 eV range. The experimental weak plateau at 10.24 eV could in principle be correlated with the theoretical peak at 9.83 eV. However, the 9.83 eV theoretical peak is more likely involved in the shoulder of the broad band at lower binding energies and, in our opinion, no theoretical peak actually correlates with the plateau at 10.24 eV. In the same way, the two "possible" (in the words of Berkowitz) weak peaks around 12.4 eV have no correspondence in the theoretical spectrum. That the absence in the VEH theoretical spectrum of metal-free phthalocyanine of the two peaks at ~ 12.4 and the peak at 10.24 eV is correct, is supported as follows:

(i) As Berkowitz points out in the case of CoPc, the appearance of these peaks in the experimental spectrum can be related with the presence of phthalonitrile due to some thermal decomposition of phthalocyanine; the photoelectron spectrum of phthalonitrile precisely presents very intense bands at 10.5 and 12.5 eV.[13]

(ii) These peaks are not detected in all the MPc molecules studied by Berkowitz.

(iii) Most importantly, no photoemission is detected at those energies in the solid state UPS spectrum of H_2Pc [see Table III and Ref. 12(c)].

On the other hand, the theoretical spectrum supports the existence of a double peak structure (11.06 and 11.74 eV) around the possible peak experimentally suggested at 11.2 eV. We have a series of reasons that confirm the existence and correct location of that double peak structure:

(i) These two peaks can be attributed (see Sec. III A) to the benzene $1a_{2u}$ and $2e_{2g}$ orbitals and the VEH energies for these levels are in very good agreement with experiment (see Table II).

(ii) A broad peak appears at ~ 11.5 eV in the experimental spectra of all metallophthalocyanines reported by Berkowitz.

(iii) A photoemission band centered between both peaks at 11.5 eV is found in the solid-state UPS spectrum of H_2Pc.[12(c)]

All the theoretical predictions for the upper part of the photoemission spectra are quantitatively confirmed by the solid-state synchrotron (photon energy = 100 eV) UPS spectrum.[12(c)] As a result, we directly compare the rest of the VEH spectrum with the solid-state data in Table III. The solid-state band peaking at 14.1 eV and corresponding to the most intense VEH peak structure G possesses a shoulder at 15.8 eV, which correlates with the single theoretical peak at 16.04 eV. The following UPS band is located at 18.5 eV just between the two theoretical peaks constituting structure E. The fact that no experimental band is detected around 20–21 eV to correlate with theoretical structure D can be explained by the low intensity of the peaks involved in that structure (see Fig. 2). The three UPS bands of highest binding energies correspond to structures C, B, and A, respectively. Structures C and A are in good agreement with experimental binding energies but structure B is calculated to be at higher binding energies. This discrepancy is understood on the basis that structure B mainly comes from the $1a_{1g}$ molecular orbitals of the benzene moieties and the binding energy of these orbitals is overestimated by the VEH method, as discussed before.

In summary, we can say that the VEH DOVS curves are fully consistent with the solid-state UPS ($h\nu = 100$ eV)

spectrum of Tegeler *et al.* and allows for a complete interpretation of the more resolved He–I UPS spectrum of Berkowitz.

IV. CONCLUSIONS

Using a VEH pseudopotential technique, we have calculated the electronic structure of metal-free phthalocyanine and discussed the theoretical simulation of the photoemission UPS and XPS spectra. The detailed analysis of the molecular orbitals of H_2Pc reveals that the electronic characteristics of the benzene moieties are conserved in the phthalocyanine macrocycle. Thus, the electronic structure of phthalocyanine must be viewed as the result of joining four benzene rings to the central carbon–nitrogen methineimine-like macrocycle rather than that of combining four isoindole units through nitrogen bridges.

The VEH one-electron energies obtained for small molecular components of phthalocyanine such as benzene, pyrrole, and isoindole are in very good agreement with experimental ionization potentials and validate the results obtained for metal-free phthalocyanine. On this basis, the VEH-calculated DOVS spectrum of H_2Pc has been correlated with the experimental gas-phase and solid-state UPS spectra. An excellent *quantitative* agreement is found between theory and experiment. The VEH predictions allow for a complete interpretation of the gas-phase spectrum and are fully supported by the solid-state data. In a forthcoming publication,[42] we intend to compare the electronic structure of phthalocyanine with that of related macrocycles, such as porphyrin, tetrabenzoporphyrin, and tetraazaporphyrin.

ACKNOWLEDGMENTS

One of us (E. O.) wishes to thank the Facultés Notre-Dame de la Paix de Namur (FNDP) for hospitality and financial support. He is also indebted to the Consellería de Cultura, Educación y Ciencia de la Generalitat Valenciana for a Postdoctoral Grant. The authors acknowledge stimulating discussions with J. M. André, J. Delhalle, B. Thémans, J. G. Fripiat, S. Stafström, H. Nakanishi, and H. Matsuda. They are indebted to FNDP, IBM-Belgium, and the Belgian National Fund for Scientific Research (FNRS) for the use of the Namur Scientific Computing Center.

[1]For recent reviews, see J. Simon and J.-J. André, *Molecular Semiconductors* (Springer, Berlin, 1985), Chap. III; *The Phthalocyanines*, edited by F. H. Moser and A. L. Thomas (Chemical Rubber, Cleveland, 1983); B. D. Berezin, *Coordination Compounds of Porphyrins and Phthalocyanines* (Wiley, New York, 1981).

[2]For a recent review on phthalocyanine applications see A. B. P. Lever, M. R. Hempstead, C. C. Leznoff, W. Lin, M. Melnik, W. A. Nevin, and P. Seymour, Pure Appl. Chem. **58**, 1467 (1986).

[3]F. Gutmann and L. E. Lyons, *Organic Semiconductors* (Wiley, New York, 1967); H. Meier, *Organic Semiconductors* (Verlag Chemie, Weinheim, 1974).

[4]A. Gleizer, T. J. Marks, and J. A. Ibers, J. Am. Chem. Soc. **97**, 3545 (1975).

[5]For a review, see (a) B. M. Hoffman and J. A. Ibers, Acc. Chem. Res. **16**, 15 (1983); (b) T. J. Marks, Science **227**, 881 (1985).

[6]P. L. Johnson, T. R. Koch, and J. M. Williams, Acta Crystallogr. Sect. B **33**, 1293 (1977).

[7]A. Pullman and G. Berthier, C. R. Acad. Sci. (Paris) **236**, 1494 (1953).

[8]S. Basu, Ind. J. Phys. **28**, 511 (1954); M. Gouterman, G. H. Wagniere, and L. L. Snyder, J. Mol. Spectrosc. **11**, 103 (1963); I. Chen, *ibid.* **23**, 131 (1967); I. Chen and M. Abkowitz, J. Chem. Phys. **50**, 2237 (1969).

[9]A. M. Schaffer and M. Gouterman, Theor. Chim. Acta **25**, 62 (1972); L. Edwards and M. Gouterman, J. Mol. Spectrosc. **33**, 292 (1970); A. M. Schaffer, M. Gouterman, and E. R. Davidson, Theor. Chim. Acta **30**, 9 (1973).

[10]C. Weiss, H. Kobayashi, and M. Gouterman, J. Mol. Spectrosc. **16**, 415 (1965); **33**, 292 (1970); A. Henriksson and M. Sundbom, Theor. Chim. Acta **27**, 213 (1972); A. Henriksson, B. Roos, and M. Sundbom, *ibid.* **27**, 303 (1972); A. J. McHugh, M. Gouterman, and C. Weiss, Jr., *ibid.* **24**, 346 (1972).

[11]L. K. Lee, N. H. Sabelli, and P. R. LeBreton, J. Phys. Chem. **86**, 3926 (1982).

[12](a) H. Höchst, A. Goldmann, S. Hüfner, and H. Malter, Phys. Status Solidi B **76**, 559 (1976); (b) F. L. Battye, A. Goldmann, and L. Kasper, *ibid.* **80**, 425 (1977); (c) E. Tegeler, M. Iwan, and E.-E. Koch, J. Electron Spectrosc. Relat. Phenom. **22**, 297 (1981), and references therein.

[13]J. Berkowitz, J. Chem. Phys. **70**, 2819 (1979).

[14]Z. Berkovitch-Yellin and D. E. Ellis, J. Am. Chem. Soc. **103**, 6066 (1981).

[15]F. W. Kutzler and D. E. Ellis, J. Chem. Phys. **84**, 1033 (1986).

[16]G. Nicolas and Ph. Durand, J. Chem. Phys. **70**, 2020 (1979); **72**, 453 (1980).

[17]J. M. André, L. A. Burke, J. Delhalle, G. Nicolas, and Ph. Durand, Int. J. Quantum Chem. Symp. **13**, 283 (1979).

[18]J. L. Brédas, R. R. Chance, R. Silbey, G. Nicolas, and Ph. Durand, J. Chem. Phys. **75**, 255 (1981).

[19]J. L. Brédas, B. Thémans, and J. M. André, J. Chem. Phys. **78**, 6137 (1983); J. L. Brédas, R. Silbey, D. S. Boudreaux, and R. R Chance, J. Am. Chem. Soc. **105**, 6555 (1983).

[20]J. L. Brédas, R. R. Chance, R. Silbey, G. Nicolas, and Ph. Durand, J. Chem. Phys. **77**, 371 (1982).

[21]J. L. Brédas, R. L. Elsenbaumer, R. R. Chance, and R. Silbey, J. Chem. Phys. **78**, 5656 (1983).

[22]J. L. Brédas and G. B. Street, J. Chem. Phys. **82**, 3284 (1985).

[23]J. L. Brédas and W. R. Salaneck, J. Chem. Phys. **85**, 2219 (1986).

[24]U. Gelius, in *Electronic Spectroscopy*, edited by D. A. Shirley (North-Holland, Amsterdam, 1972), p. 311.

[25]R. S. Mulliken, J. Chem. Phys. **23**, 1833 (1955).

[26]J. M. Robertson, J. Chem. Soc. **1935**, 615.

[27]J. M. Robertson, J. Chem. Soc. **1936**, 1195.

[28]B. F. Hoskins, S. A. Mason, and J. C. B. White, J. Chem. Soc. Chem. Commun. **1969**, 554.

[29]E. B. Fleischer, Acc. Chem. Res. **3**, 105 (1970).

[30]Y. Niwa, H. Kobayashi, and T. Tsuchiya, J. Chem. Phys. **60**, 799 (1974); Inorg. Chem. **13**, 2891 (1974).

[31]L. Nygaard, J. J. Nielsen, J. Kirchheiner, G. Maltesen, J. Rastrup-Andersen, and G. O. Sorensen, J. Mol. Struct. **3**, 491 (1969).

[32]A. Langseth and B. P. Stoicheff, Can. J. Phys. **34**, 350 (1956).

[33]G. A. Williams, B. N. Figgis, R. Mason, S. A. Mason, and P. E. Fielding, J. Chem. Soc. Dalton Trans. **1980**, 1688.

[34]B. H. Meier, C. B. Storm, and W. L. Earl, J. Am. Chem. Soc. **108**, 6072 (1986).

[35]U. Gelius, C. J. Allan, G. Johansson, H. Siegbahn, D. A. Allison, and K. Siegbahn, Phys. Scr. **3**, 237 (1971).

[36]W. von Niessen, L. S. Cederbaum, and W. P. Kraener, J. Chem. Phys. **65**, 1378 (1976).

[37]W. von Niessen, L. S. Cederbaum, and G. H. F. Diercksen, J. Am. Chem. Soc. **98**, 2066 (1976).

[38]See, for example, L. Klasinc, A. Sabljic, G. Kluge, J. Rieger, and M. Scholz, J. Chem. Soc. Perkin Trans. 2 **1982**, 539.

[39]W. Rettig and J. Wirz, Helv. Chim. Acta **59**, 1054 (1976).

[40]J. Almlöf, Int. J. Quantum Chem. **8**, 915 (1974); R. E. Christoffersen, *ibid.* **16**, 573 (1979); U. Nagashima, T. Takada, and K. Ohno, J. Chem. Phys. **85**, 4524 (1986).

[41]A. Case and M. Karplus, J. Am. Chem. Soc. **99**, 6182 (1977).

[42]E. Ortí and J. L. Brédas (to be published).